JOURNAL OF NANO- AND ELECTRONIC PHYSICS
Vol. 7 No 1, 01028(5pp) (2015)

ЖУРНАЛ НАНО- ТА ЕЛЕКТРОННОЇ ФІЗИКИ
Том 7 № 1, 01028(5cc) (2015)

Effect of Hydrothermal Treatment on the Phase Composition of Titanium Dioxide Obtained by $Ti(OC_4H_9)_4$ Hydrolysis

M.G. Mizilevska[1], V.O. Kotsyubynsky[2], O.H. Tadeush[1]

[1] *South Ukrainian National Pedagogical University named after K.D. Ushynsky,*
26, Staroportofrankivs'ka Str., 65020 Odesa, Ukraine
[2] *Vasyl Stefanyk Precarpathian National University, 57, Shevchenko Str., 76018 Ivano-Frankivsk, Ukraine*

(Received 20 November 2014; revised manuscript received 25 November 2014; published online 25 March 2015)

The use of hydrothermal treatment of amorphous material obtained by hydrolysis of titanium tetrabutoxide provides a nanostructured mixture of anatase and brookite – photocatalytic active phases of titanium dioxide, which are characterized by thermal stability to the phase transformation to rutile if particle size is about 4 nm and value of the specific surface area is 175 m²/g.

Keywords: Brookite, Anatase nanoparticles, Phase transformation, Tetrabutoxide titanium, Hydrothermal treatment.

PACS numbers: 61.46. – w , 61.82.Rx x

1. INTRODUCTION

Titanium dioxide exists in three modifications, such as, anatase, brookite, and rutile. Anatase (tetragonal structure, D_{4h}^{19} symmetry group) is irreversibly transformed into rutile (tetragonal structure, symmetry group D_{4h}^{14}) upon heating, and transition temperature is determined by its morphological characteristics [1]. Metastable phase of brookite (rhombohedral structure, D_{4h}^{15} symmetry group) is relatively poorly studied, although its higher photocatalytic activity in comparison with anatase is noted in a number of works, in particular [2]. Surface energy of brookite particles is 2.5 times larger than of anatase ones (1.0 ± 0.2 and 0.4 ± 0.1 J/m², respectively) [3]. In the majority of the cases, brookite is obtained in the hydrothermal conditions at temperatures of 100-200 °C [4]. Monophase brookite with submicron crystallites is typically obtained by the hydrothermal method at relatively high temperatures and pressure ($P = 1$-40 MPa and $T = 200$-400 °C) [5]. At the same time, formation of brookite as an impurity in the synthesis of anatase by the sol-gel method was noticed in a number of publications, in particular [6-11].

Functional properties of titanium dioxide are determined by its phase composition, degree of dispersity, and morphology of particles. Modern chemical technologies allow to obtain this material in the form of a porous xerogel, aerogel, spherical particles, bars, fibers, or tubes with the structure of anatase, brookite, and rutile [12-16], at that different modifications of the sol-gel method took the first place among the controlled synthesis methods. Generally, sol-gel method includes the formation of metaloxypolymer chains – sol or gel from soluble polyhydroxocomplexes formed as a result of hydrolysis of metal-organic complex or inorganic compounds. Change in the reaction parameters (reaction time, temperature, concentration, and chemical composition of reagents) allows to control the characteristics of the final product. Control of the behavior of the polycondensation processes in a sol plays the key role in obtaining nanostructures with the specified characteristics, since the morphological characteristics and phase composition of titanium dioxide are determined just on this stage.

Titanium alcoholates are the universal precursors in the sol-gel synthesis of TiO_2 [17, 18]. Absence of foreign cations in the reaction medium is their main advantage, while molecules of alcohols can be comparatively easily removed by washing or thermal treatment. An additional advantage is the possibility to vary the velocities of hydrolysis and polycondensation by the change in the concentration of nucleophilic reagents. Moreover, the reactivity of alcoholates can be varied by the formation of the mixed-ligand complexes [19].

The possibility to control the phase composition of the hydrated titanium dioxide obtained by the hydrolysis of titanium tetrabutoxide by the change in the acidity of the reaction medium is stated in the work [20]. The authors of [21] have established that for the values of $pH < 0.25$ in the diluted acidic solutions, amorphous hydrated TiO_2 is crystallized in the form of rutile, and for $0.75 < pH < 0.9$ nuclei of anatase and brookite phases are formed simultaneously.

Decrease in the crystallite sizes of both polymorphs with decreasing hydrolysis and thermal treatment temperature is interpreted as a consequence of the presence on the material surface of chemisorbed OH-groups whose occurence slows down the grain growth.

The aim of the performed investigations was to determine the influence of the synthesis conditions on the phase composition and morphological characteristics of ultradispersed TiO_2 by the hydrolysis method of titanium tetrabutoxide and study of the obtained material by the methods of the X-ray structural analysis, derivatographic analysis and adsorption porometry.

2. EXPERIMENTAL

2.1 Features of the synthesis of nanoporous and nanostructured titanium dioxides

Formation of the titanium hydroxide precipitate in the deposition of alkali diluted solutions of Ti(IV) salts at room temperature occurs at $pH = 1.4$. As-deposited titanium hydroxide is the compound of variable composition with the most probable formula $TiO(OH)_2 \cdot nH_2O$ (there are several other points of view according to which formula $Ti(OH)_4$ or $TiO(OH)_2$ is ascribed to titanium hydroxide) [22]. $Ti(OH)_3^+$ and $Ti(OH)_2^{2+}$ are the main hydroxocomplex compounds of Ti(IV) which are in the equilibrium with the deposited hydroxide phase.

Monomeric hydrolyzed ions exist only in very dilute solutions. Behavior of the hydrolysis processes and further hydrolytic polycondensation (on account of olation and oxolation reactions) leads to the formation of polynuclear titanium hydroxocomplexes as evidenced by a slow decrease in pH during aging of solutions and deposition of titanium hydroxide. Henceforth, polynuclear complexes with a decreased solubility grow to the sizes of colloidal particles [23]. It was noted that particles of titanium hydroxide obtained by the sol-gel method of the spherical shape and size of about 100 nm are composed of closely packed primary amorphous particles of the size of 2-3 nm [24].

Advantages of the application of titanium alkoxides as the precursors in the sol-gel synthesis of TiO_2 led to active investigations of the behavior of $Ti(OR)_4$ hydrolysis reactions [18]. For the case of titanium tetrabutoxide, schematic hydrolysis reaction can be described as $Ti(OC_4H_9)_4 + 4H_2O \rightarrow Ti(OH)_4 + 4C_4H_9OH$, however, it does not represent the aggregation of hydrocomplexes in polycondensation with participation of OH-groups [17]. If polycondensation reaction occurs simultaneously with hydrolysis, an morphous product is typically formed, the reason being the inhibitory influence of alkyls.

2.2 Synthesis process

The first stage of titanium dioxide synthesis provided for hydrolysis of titanium tetrabutoxide in the mixture of anhydrous ethanol, nitric acid, and distilled water. Solution of titanium tetrabutoxide in anhydrous ethanol (the finite value is pH = 4) was prepared. Aqueous solution of ethanol, nitric acid and PEG300 (the finite value is pH = 0.9) was prepared simultaneously and added drop by drop to the solution of titanium tetrabutoxide under the condition of intense mixing. The finite pH value of the reaction medium was equal to 0.9. Volume ratio of the components was $C_{16}H_{36}O_4Ti : C_2H_5OH : HNO_3 : H_2O$: PEG300 = 1 : 15 : 0.3 : 4 : 0.004. Results of the work [25] were used when planning the experiment.

The obtained mixture was blended during 2 hours to the formation of a precipitate. Concentration of nitric acid was the control factor and accelerated hydrolysis simultaneously slowing down the polycondensation reaction. Low values of pH of the reaction medium increased the aggregation stability of a sol.

At the second stage, two options to continue synthesis were applied. In the first case, precipitate was separated from the mother solution by centrifugation and repeatedly dispersed in ethanol to minimize agglomeration of particles. In the second case, its hydrothermal treatment was performed: the initial solution containing amorphous precipitate was placed into autoclave with teflon coating and kept at the temperature of 160 °C during 5 hours. After hydrothermal treatment suspension was centrifuged; the separated material was washed by ethanol and dried at the temperature of 60-70 °C.

Two series of the samples were synthesized: system A (materials obtained under the condition of hydrothermal treatment) and system B (materials obtained under the condition of sol deposition).

3. RESULTS AND DISCUSSION

X-ray diffraction investigations of the obtained samples were carried out using diffractometer DRON-4-07 with the X-ray beam focusing by the Bragg-Brentano scheme in the radiation of copper anode ($\lambda = 1.54178$ Å) and Ni-filter.

Analysis of the diffraction patterns of the systems A and B has shown that mixtures of anatase and brookite phases were obtained in both cases. An exact analytical separation of the basic reflexes of anatase and brookite ((110), (120) and (111), respectively), which are overlapped in the vicinity of $2\theta = 25°$, for the case of a nanocrystalline material is problem, however, changes in the content of brookite are clearly fixed by the reflex (121) at $2\theta = 30.81°$ (Fig. 1). It is established that material of the system A obtained using hydrothermal treatment is characterized by a relatively large content of brookite.

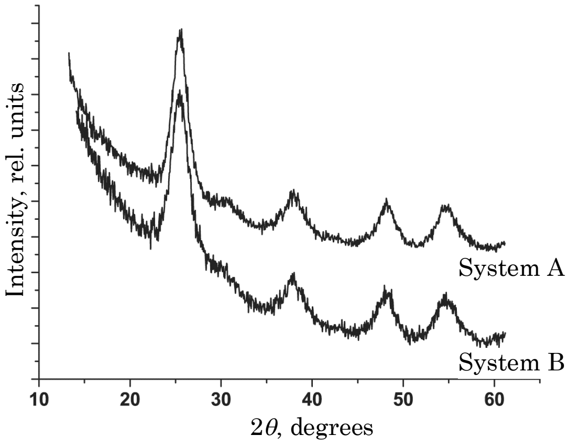

Fig. 1 – Diffraction patterns of the initial TiO_2 samples of the systems A and B

Presence of broadening of reflexes on the diffraction patterns (Fig. 1) indicates the dispersion of the material. The average particle size L was calculated using the Scherrer formula $L = \lambda/\Delta(2\theta)\cos\theta_0$ [26], where λ is the X-ray wavelength; $\Delta(2\theta)$ is the half-height peak width; θ is the diffraction angle. As the calculation results have shown, average size of anatase particles for the initial materials of the systems A and B are equal to about 4.3 and 3.4 nm, respectively.

Thermal derivatographic investigation of the obtained materials was carried out using thermal analyzer STA 499 F3 JUPITER in the temperature range of 20-800 °C. Activation energies were calculated based on the analysis of the DTA curves by the technique [27].

For the material of the system A, mass loss in the temperature range of 52-770 °C (Fig. 2) was approximately equal to 18.5 %. The main stage of mass loss (about 7.7 %) is completed at the temperature of about 160 °C and corresponds to the material dehydration. The process has endothermic behavior (activation energy is equal to 72 kJ/mole) with the heat absorption maximum in the vicinity of the temperature of 102 °C. The residual loss of bound water (to 6 %) is observed in the temperature range of 158-300 °C. Two exothermal effects with maxima at the temperatures of 449 and 502 °C, respectively, are registered in the temperature range of 300-606 °C, which are accompanied by the loss to 4.8 % and correspond to the anatase-rutile phase transition.

Total mass loss for the material of the system B was 23.58 % (Fig. 3), at that about 22 % was lost during the endothermic process (activation energy is 28 kJ/mole) with maximum at 138 °C. In the temperature range of 220-604 °C, there occurred the exothermic process with maximum at 320 °C conditioned by the anatase-rutile phase transition; and 1.56 % of the mass was lost during this transition. Mass loss was completed at 540 °C. One more endothermic process, which was not accompanied by the changes in the sample mass, was observed in the vicinity of 700 °C.

Thus, differences in the behavior of the materials of the systems A and B at higher temperatures are observed under the same conditions of the thermal-induced processes on the initial annealing stage. To explain the fixed result, X-ray structural investigations of the materials obtained by annealing of the samples of the systems A and B during 1 hour at the temperatures of 200, 400 and 600 °C, respectively, have been performed.

X-ray phase analysis of the samples of the system A (Fig. 4) has shown that materials obtained by annealing at the temperatures of 200 and 400 °C remain the mixture of anatase and brookite phases. At this, weak and narrow peak is fixed at $2\theta = 31.3°$ and its presence goes beyond the error of the experiment which can be assigned to the reflex (121) of the brookite phase [28]. Thus, insignificant amount of brookite nanocrystallites in the material grows actively even at a relatively low annealing temperature of 200 °C. At the same time, growth of relative content of anatase phase (to 64 %) is observed during annealing at this temperature. This can be explained by the fact that a part of anatse is in the form of poorly crystalline particles which are recrystallized during annealing. Increase in the temperature of thermal treatment to 400 °C induces the growth of a relative content of the brookite phase (to 56 %). Obviously, the anatase-brookite phase transition is observed; however, presence of the rutile phase is not fixed. Based on the estimation of the changes in the width of reflexes, one can state that average size of the material particles is slightly varied and lies within 4 nm. Phase transition of a part of brookite and anatase into rutile, whose content exceeds in this case 40 % (Fig. 4), occurred after annealing at the temperature of 600 °C. At the same time, growth of the anatase and brookite particle sizes to 10-15 nm is fixed.

X-ray phase analysis of the annealed samples of the system B (Fig. 5) has shown that at the temperature of 200 °C the material, as well as in the case of the system A, is the mixture of the anatase and brookite phases, however, active growth of a part of crystallites of the latter was not fixed (Fig. 4).

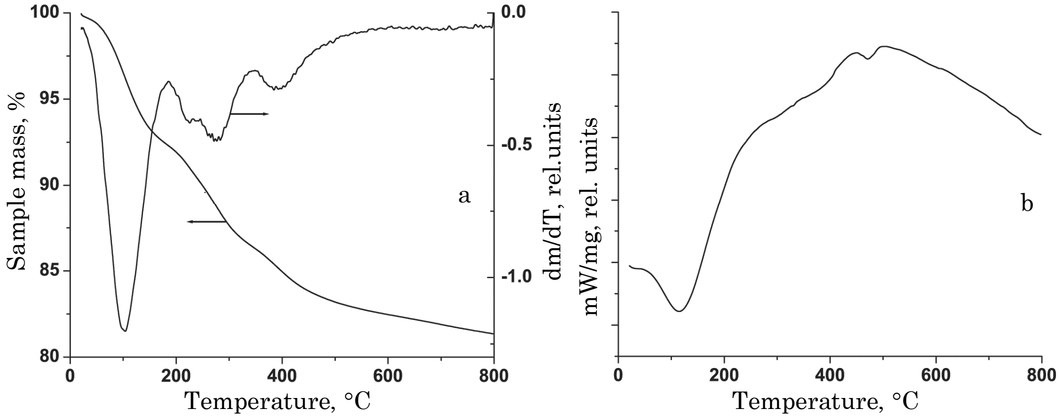

Fig. 2 – Results of the thermogravimetric, differential-thermogravimetric (a) and differential-thermal (b) analysis for the initial sample of the system A

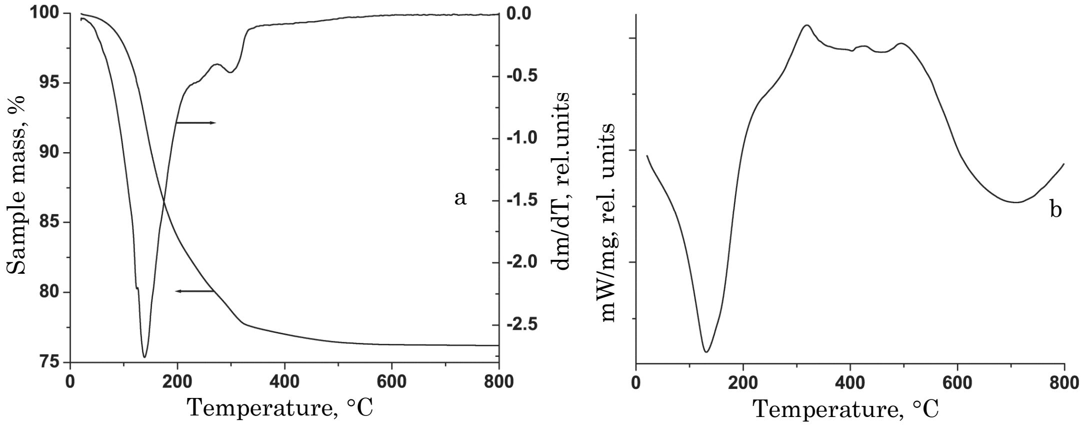

Fig. 3 – Results of the thermogravimetric, differential-thermogravimetric (a) and differential-thermal (b) analysis for the initial sample of the system B

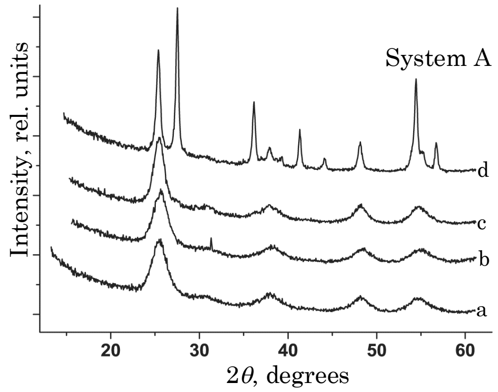

Fig. 4 – Diffraction patterns of the samples of the system A: initial (a) and obtained by annealing in air during 1 hour at the temperatures of 200 (b), 400 (c) and 600 °C (d)

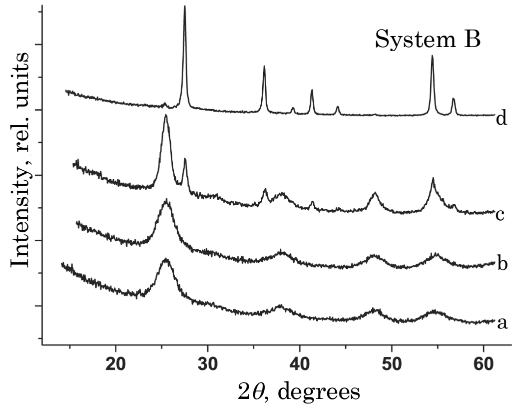

Fig. 5 – Diffraction patterns of the samples of the system B: initial (a) and obtained by annealing in air during 1 hour at the temperatures of 200 (b), 400 (c) and 600 °C (d)

Increase in the relative content of the anatase phase with no changes in the average size of its crystallites is observed similarly to the above considered case. Situation is changed for the material of the system B obtained by annealing at the temperature of 400 °C, in the phase composition of which 15-17 % of rutile is fixed.

The following model can be proposed for the interpretation of the obtained result. In the first case, brookite is present in the form of separate particles that confirms the existence of the reflex at $2\theta = 31.3°$. This is promoted by the hydrothermal processing conditions, at which probability of the realization of thermodynamically unstable phase configurations increases [29]. In the second case, situation when anatase and brookite phases coexist within a particle is a dominant one. According to the data of [30], nuclei of the brookite phase which are formed on the surfaces (112) of anatase crystallites become the areas, where the anatase-rutile transition begins. Thus, phase stability of the obtained material is less. A similar result was obtained by the authors of [31]. For the sample of the system B obtained by annealing at the temperature of 600 °C, rutile of the particles of 25-30 nm is an absolutely dominant phase, and content of the anatase phase does not exceed 2-3 %. The above considerations agree completely with the investigation results of the structural-absorption characteristics of the materials of the studied systems. Nitrogen absorption method at 77 K (sorbometer Quantachrome Autosorb Nova 2200e) was applied. Specific surface area of the initial materials of the systems A and B was equal to 60 and 10 m^2/g, while annealing at the temperature of 200 °C led to the increase in the specific surface area to 175 and 107 m^2/g, respectively.

4. CONCLUSIONS

Using methods of the X-ray structural analysis, thermogravimetry and adsorption porometry, it is established that hydrothermal treatment of the hydrolysate – titanium tetrabutoxide – followed by annealing at temperatures to 400 °C allows to obtain the nanostructured composite of the anatase/brookite phases with the specific surface area to 175 m^2/g. It is found that the obtained material is characterized by the phase stability of the anatase/brookite $\rightarrow$ rutile transition that can be used in the design of materials for photocatalytic applications.

REFERENCES

1. D.A.H. Hanaor, C.C. Sorrell, *J. Mater. Sci.* **46**, 855 (2011).
2. W.-K. Li, X.-Q. Gong, G. Lu, A. Selloni, *J. Phys. Chem. C* **112**, 6594 (2008).
3. M.R. Ranade, A. Navrotsky, H.Z. Zhang, *PNAS* **99**, 6476 (2002).
4. J. Xie, X. Lü, J. Liu, H. Shu, *Pure Appl. Chem.* **81**, 2407 (2009).
5. Z. Keesmann, *Z. Anorg. Allg. Chem.* **346**, 30 (1966).
6. C.C. Wang, J. Ying, *Chem. Mater.* **11**, 3113 (1999).
7. Q. Zhang, L. Gao, *Langmuir* **19**, 967 (2003).
8. P. Arnel, R.J.P. Corriu, l. Leclercq, P.H. Mutin, A. Vioux, *J. Mater. Chem.* **6**, 1925 (1996).
9. Y. Djaoued, R. Bruning, D. Bersani, P.P. Lottici, S. Badilescu, *Mater. Lett.* **58**, 2618 (2004).
10. A. Pottier, C. Chaneac, E. Tronc, L. Mazerlolles, J.P. Jolivet, *J. Mater. Chem.* **11**, 1116 (2001).
11. S.L. Isley, R.L. Penn, *J. Phys. Chem. B* **110**, 15134 (2006).
12. M.R. Ayers, A.J. Hunt, *Mater. Lett.* **34**, 290 (1998).
13. A. José Rodríguez, Marcos Fernández-García, *Synthesis, properties, and applications of oxide nanomaterials*. (Hoboken: Wiley-Interscience a John Wiley & Sons: 2007).
14. A. Chemseddine, T. Moritz, *Eur. J. Inorg. Chem.* **1999**, 235 (1999).
15. X. Chen, S.S. Mao, *Chem. Rev.* **107**, 2891 (2007).
16. T. Kasuga, M. Hiramatsu, A. Hoson, *Langmuir* **14(12)**, 3160 (1998).
17. M. Gobal, W.J. Moberly Chan, L.C. De Jonghe, *J. Mater. Sci.* **32**, 6001 (1997).
18. C.J. Brinker, G.W. Scherer, *Sol-Gel Science: The Physics and Chemistry of Sol-Gel Processing* (Boston: Academic Press: 1990).
19. *Funktsional'nyye nanomaterialy* (Red. Yu.D. Tret'yakova) (Moskva: Fizmatlit: 2010).
20. J.-P. Nikkanen, *J. Cryst. Growth* **304**, 179 (2007).
21. S.G. Kumar, K. S. R. Koteswara, *Nanoscale* **6**, 11474 (2014).
22. A.Ya. Goroshchenko, *Khimiya titana. Ch. 2* (Kiev: Nauk. dumka: 1972).
23. V.V. Popov, *Obrazovaniye dispersnykh sistem oksidov, oksigidroksidov i gidroksidov elementov. Obzor* (M.: NIITEKhIM: 1991).
24. H. Zhang, M. Finnegan, J.F. Banfieid, *Nano Lett.* **1**, 81 (2000).
25. K. Yu, J. Zhao, Y. Guo, X. Ding, Y. Liu, Z. Wang, *Mater. Lett.* **59**, 2515 (2005).
26. A. Gin'ye, *Rentgenografiya kristallov. Teoriya i praktika*

(M.: Nauka: 1961).

27. *Termografiya: Metodicheskiye ukazaniya po distsipline "Fiziko-khimicheskiye metody issledovaniya"* (Sost. L.N. Pimenova) (Tomsk: Izd-vo Tomsk. arkhit.-stroit. un-ta: 2005).
28. H. Zhang, J.F. Banfield, *J. Phys. Chem. B* **104**, 3481 (2000).
29. Li Ji-Guang, T. Ishigaki, X. Sun, *J. Phys. Chem. C* **111**, 4969 (2007).
30. M. Rezaee, S.M.M. Khoie, Kun Hua Liu, *Cryst. Eng. Comm* **13**, 5055 (2011).
31. J. Ovenstone, K. Yanagisawa, *Chem. Mater.* **11**, 2770 (1999)..